J Mater Sci (2007) 42:3951–3957
DOI 10.1007/s10853-006-0166-9

$L1_2$-phase cutting during high temperature and low stress creep of a Re-containing Ni-base single crystal superalloy

A. Kostka · G. Mälzer · G. Eggeler · A. Dlouhy · S. Reese · T. Mack

Received: 5 December 2005 / Accepted: 3 April 2006 / Published online: 31 January 2007

Abstract In the present study, we investigate dislocation processes in a Ni-base single crystal superalloy (LEK94) after high temperature and low stress creep. Specimens were creep deformed at 240 MPa and 980 °C to a strain of 20%. We use diffraction contrast transmission electron microscopy (TEM) to show that two γ-channel dislocations with different Burgers vectors combine and form a super dislocation that shears the γ'-particle. This type of cutting event has now been observed for three single crystal superalloys with different alloy chemistry (CMSX-4, CMSX-6 and LEK94 in the present work) and we therefore conclude that it represents a generic elementary dislocation process which governs high temperature (around 1000 °C) and low stress (around 240 MPa) creep. The present paper provides microstructural evidence for this type of cutting processes and discusses the results in the light of previous work published in the literature.

A. Kostka (✉) · G. Mälzer · G. Eggeler
Institut für Werkstoffe, Ruhr-Universität Bochum, Bochum 44780, Germany
e-mail: Alexander.Kostka@rub.de

A. Kostka
Institute of Materials Science, University of Silesia, Katowice 40-007, Poland

A. Dlouhy
Institute of Physics of Materials, Academy of Sciences of the Czech Republic, Brno 616 62, Czech Republic

S. Reese
Institut für Mechanik, Ruhr-Universität Bochum, Bochum 44780, Germany

T. Mack
MTU Aero Engines GmbH, Dachauer Str. 665, München 80995, Germany

Introduction

Superalloy single crystals are used to make turbine blades. Single crystal turbine blades represent critical components in gas turbines, which limit the gas inlet temperature and thus the thermal efficiency of the engine. Turbine blades must withstand the most severe operating conditions that include creep stresses of the order of 100 MPa at temperatures up to 1100 °C. Their mechanical performance at high temperature limits the service life of the gas turbine [e.g. 1–3].

It is well known that the microstructure of single crystal superalloys consists of γ'-cubes (ordered $L1_2$-phase; typical cube edge length: 0.5 μm) separated by thin γ-channels (fcc, typical width: 0.05 μm). Due to the technological importance of this microstructure its plastic deformation behaviour has received considerable attention in the scientific literature. Many transmission electron microscopy (TEM) studies focused on the evolution of microstructure in the low temperature (up to 800 °C) high stress range (500 MPa and more). Associated dislocation processes like the filling of γ-channels with dislocations [e.g. 4, 5] or the pair wise cutting of the γ'-particles by two normal $a_0/2\ \langle 110\rangle$ dislocations which move by glide and are coupled by an antiphase boundary (APB) [e.g. 6–9] are prominent results of plasticity research.

While there has been a strong focus on low temperature high stress creep of superalloy single

crystals, creep deformation mechanisms at higher temperatures and lower stresses have only recently received attention [e.g. 5, 10–17]. Creep under high temperature and low stress conditions is governed by a number of elementary processes which include the filling of γ-channels with dislocations, recovery processes at γ'-cube corners (in the early stages of rafting), rafting (where for negative misfit alloys γ'-cubes coarsen into γ'-rafts oriented perpendicular to the direction of the maximum principal stress) and γ'-cutting; a description of the interaction of these elementary processes has been given by Kamaraj et al. [18].

As a striking new result, it was found that at high temperatures and low stresses γ'-cutting is accomplished by non octahedral superdislocations with Burgers vectors of type a_0 ⟨100⟩. Louchet and Ignat [10] and Bonnet and Ati [11] had already observed a_0 ⟨100⟩ dislocations after high temperature and low stress creep in the single crystal superalloy CMSX-4. But, they did not relate this observation to dislocation plasticity in the γ/γ'-microstructure. Eggeler and Dlouhy [12] showed that these a_0 ⟨100⟩ dislocations result from a reaction between two channel dislocations with different Burgers vectors (''**b**s'') which move by a combined process of glide and climb. They performed a diffraction contrast study on the single crystal superalloy CMSX-6 after creep at 1025 °C and 85 MPa. They provided clear evidence for this cutting process. In Fig. 2a of their paper the upper of two channel dislocations which jointly shear the γ'-particle is invisible. In their Fig. 2b, this upper dislocation is fully visible while the lower dislocation is effectively invisible. And both channel segments are visible in all other micrographs presented in Fig. 2 of their report [12]. The superdislocation in the γ'-particle was identified as having a Burgers vector of a_0 ⟨100⟩. Eggeler and Dlouhy [12] were not able to resolve the dislocation core. A subsequent dislocation contrast simulation [13] showed that dislocation contrasts were correctly interpreted in [12] but the simulations did not help to decide whether the dislocation core was compact or split. Srinivasan et al. [14] progressed the understanding of this observation in three respects. They showed that the cutting event observed by Eggeler and Dlouhy [12] was not an isolated observation related to CMSX-6 but that it also occurs in the single crystal superalloy CMSX-4 crept at 1020 °C and 80 MPa. They used high resolution transmission electron microscope (HRTEM) to show that the dislocation core of the a_0 ⟨100⟩ superdislocation is not compact but that it consists of two superpartials with different **b**s which can only move by a combined process of glide and climb. And most importantly, they related this cutting event to the creep rate of the material. They showed that secondary creep in rafted γ/γ'-microstructures can only proceed when dynamic recovery is related to this type of cutting process. This implies that dislocations on one side of a γ'-raft cut through the ordered region and annihilate with dislocations of opposite sign on the other side of the γ'-raft. Recently, Zhang et al. [16] showed that this type of γ'-cutting process, where two γ-channel dislocations with different Burgers vectors jointly shear the γ'-phase can also be observed in the Japanese single crystal super alloy TMS-138.

This observation is very important from a microstructural and from a mechanical point of view. The character of the disordered region between the two dislocations with different Burgers vectors remains to be explained. It is clear that this process differs from the well known classical cutting process where two APB-coupled superpartials (with the same Burgers vector!) jointly shear the γ'-particle, e.g. [6–8]. If the ⟨100⟩-type superdislocation cutting events govern creep in Ni-base superalloys, this certainly will affect the area of micromechanical modeling of creep. Because these implications are wide ranging, it is important to show that this cutting process represents a generic feature of high temperature and low stress creep in the whole family of Ni-based single crystal superalloys. Therefore the objective of the present study is to provide yet another example for a γ'-cutting process, where the ordered phase is cut by two γ-channel dislocations with different **b**s which form a superdislocation in the γ'-particle. We will show that this type of cutting process also occurs in the light weight Ni-base superalloy LEK94.

Material and experiment

Material

The material investigated in the present study was received as cylindrical rods with a diameter of 19 mm and had the chemical composition which is given in Table 1. It represents a low density Ni-base superalloy. Its heat treatment consisted of the usual type of increasing step annealing to dissolve coarse primary γ'

Table 1 Chemical composition of LEK 94

Element	Cr	Co	Al	Ti	Mo	Ta	W	Re	Ni
(wt-%)	6.0	7.5	6.5	1.0	2.1	2.3	3.5	2.5	Bal.

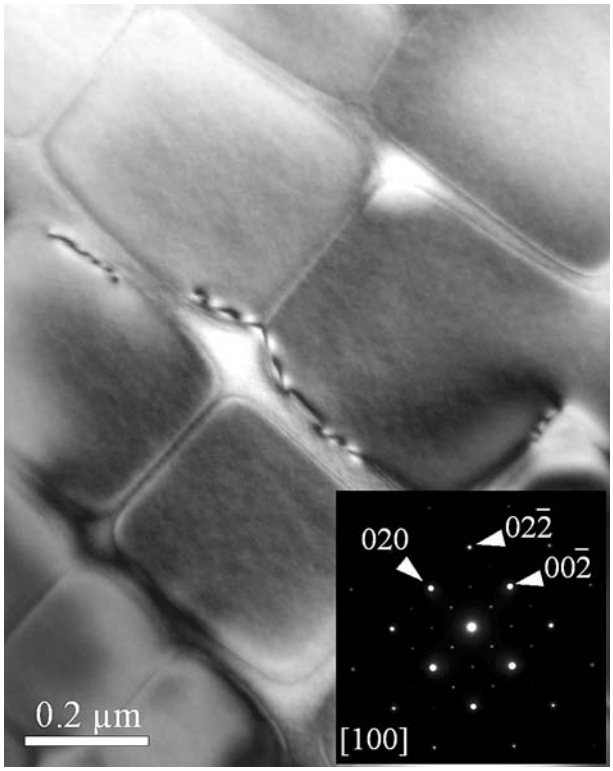

Fig. 1 TEM-micrograph of the as received material. The γ'-cubes are separated by γ-channels. The corresponding selected area diffraction pattern was obtained from a 1 μm region and contains contributions from both phases. The fine extra spots represent the ordered $L1_2$-phase

by avoiding intercipient melting. The dissolution treatment was followed by precipitation annealing for 5 h at 1080 °C and 8 h at 900 °C. The microstructure of the as received material is shown in Fig. 1.

Creep

Creep testing was performed using creep machines of type DMG (Denison Mayes Group), which were equipped with high temperature furnaces. Strain time readings were recorded using a PC-based data acquisition system. All details concerning our creep test procedure are published elsewhere [19]. Cylindrical specimens with a diameter of 5 mm and a gauge length of 25 mm were used (geometry described in [20]). The as received rods were oriented using the Laue-technique. Spark erosion machining was used to obtain ⟨100⟩ cylindrical rods (precision 1–2°) from which tensile creep specimens were obtained by turning and subsequent surface polishing. In the present study, we consider a creep condition of 980 °C and 240 MPa; rupture occurred after 125 h at a rupture strain of 20%. Slight necking was observed in the final stages of the creep process. About 5 mm of the gauge length were affected by necking (down from an initial specimen diameter of 5 mm to a diameter in the neck of 4 mm). The thin foil for the TEM investigation was taken from a gauge length region which was not affected by necking. The TEM micrograph in Fig. 2 shows the material after creep deformation to 20%. In agreement with many previous TEM studies on single crystal superalloys after creep in a similar stress and temperature regime a high dislocation density in the γ-channels can be detected (Fig. 2a) and γ'-cutting processes are observed (Fig. 2b).

Transmission electron microscopy

TEM specimens were taken from the as received rod and from the crept specimen by cutting out slices of about 0.5 mm in thickness parallel to the specimen axis using a slow diamond saw. The slices were mechanically ground to a thickness of 0.15 and 3 mm diameter discs were then stamped out. TEM foils were obtained by standard electrochemical double-jet thinning using a Struers TenuPol-5. Good thinning conditions were achieved using an electrolyte consisting of 70 vol-% methanol, 20 vol-% glycerine and 10 vol-% perchloric acid at –20 °C. The voltage was selected as 11.5 V and a flow rate of 15 was chosen. TEM was performed

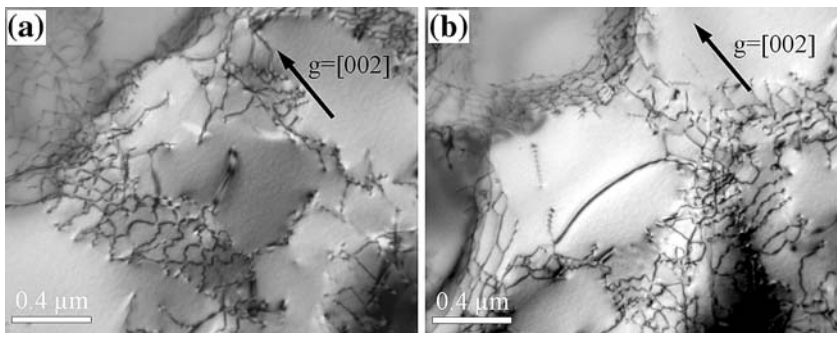

Fig. 2 TEM micrographs of the structure of the superalloy after creep. (**a**) Filling of γ-channels with dislocations; (**b**) Cutting of the γ'-particle

using a Phillips CM20 operating at 200 kV. For the objectives of the present study, it is important to investigate a location in the TEM foil where a γ'-cutting event is observed. The case which we selected for analysis is shown in Fig. 3. It can be seen that two γ-channel dislocations $d_{\gamma 1}$ and $d_{\gamma 2}$ enter and leave the γ'-precipitate which has suffered rafting. In the γ'-raft, the two dislocations form a superdislocation $d_{\gamma'}$. In the present study we investigate this cutting event using classical **g**·**b**-analysis [21, 22]. We use seven well defined two-beam conditions **g** illustrated in the schematic Kikuchi map of Fig. 4 to study this cutting process. Our TEM micrographs were taken with a small positive deviation vector **s** for the two-beam conditions **g**. The contrast conditions considered in the present study are listed in Table 3. We use a cube projection method to indicate the crystallographic orientation of the TEM specimen in the different tilt positions [23]. Kikuchi line diffraction patterns were evaluated to calculate the projected cubes [23]. In combination with stereo TEM [23], the cube projection method facilitates determination of the directions of dislocation line segments.

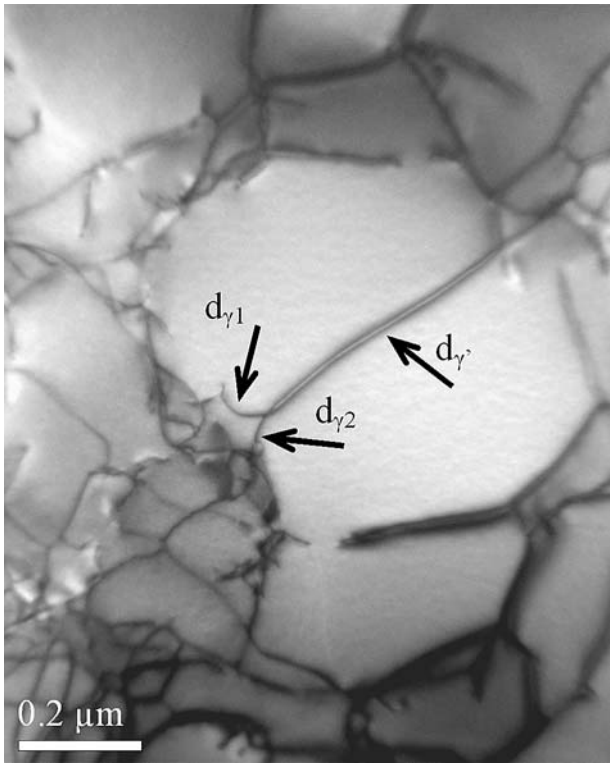

Fig. 3 TEM micrograph of the cutting event investigated in the present work (multiple beam contrast). Dislocations $d_{\gamma 1}$ and $d_{\gamma 2}$ represent γ-channel (Ni-based solid solution) dislocation segments. They form the superdislocation $d_{\gamma'}$ in the γ'-particle ($L1_2$ phase)

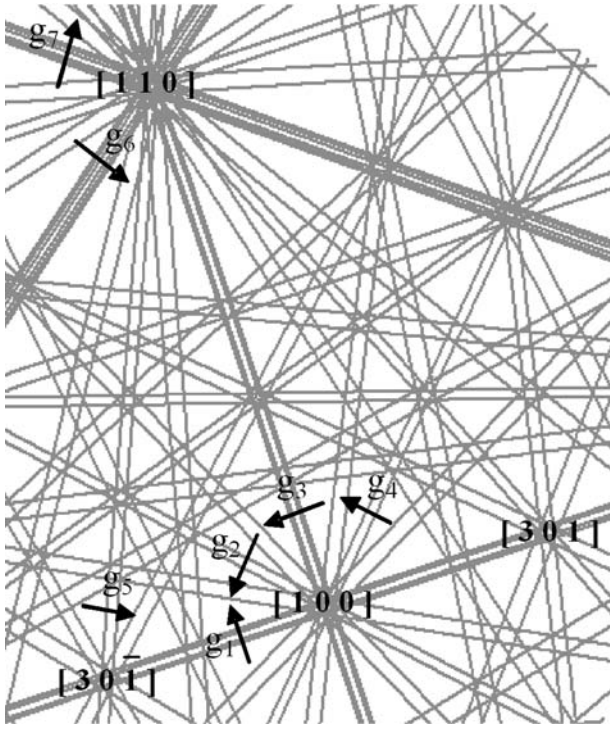

Fig. 4 Schematic Kikuchi map and corresponding two-beam conditions used in the present study

Results and discussion

Our results show that the dislocation density in the as received material is low, Fig. 1. During creep the dislocation density in the γ-channels increases, Fig. 2a. We also observe cutting processes, Figs. 2b and 3. Figure 3 shows that two γ-channel dislocations form a superdislocation and jointly shear the γ'-particle.

The seven TEM images associated with the tilt positions of Fig. 4 are presented in Fig. 5. They contain the **g**-vector and a projected cube indicating crystallographic directions. Figure 5 shows that for all tilt positions the line direction **u** of the superdislocation $d_{\gamma'}$ is parallel to the [011]-direction. The [011]-direction represents the diagonal of the upper (100)-plane of the projected cube. It is not easy to determine the dislocation line directions of the superpartials. Using stereo microscopy in combination with the cube projection method they were approximately obtained as $\mathbf{u}_{d\gamma 1} = 1/\sqrt{101}[61\bar{8}]$ and $\mathbf{u}_{d\gamma 2} = 1/\sqrt{41}[1\bar{6}2]$. The line directions of the three dislocations which characterise our cutting scenario are listed in Table 2.

In Table 3 we summarize the dislocation contrasts of the dislocation segments $d_{\gamma'}$, $d_{\gamma 1}$ and $d_{\gamma 2}$ as observed in Fig. 5. We differentiate between visibility (‘‘+’’), effective invisibility (‘‘–’’) and weak residual contrast (‘‘res’’). There are two effective invisibilities ($\mathbf{g}(\mathbf{b} \times \mathbf{u}) = 0$) for

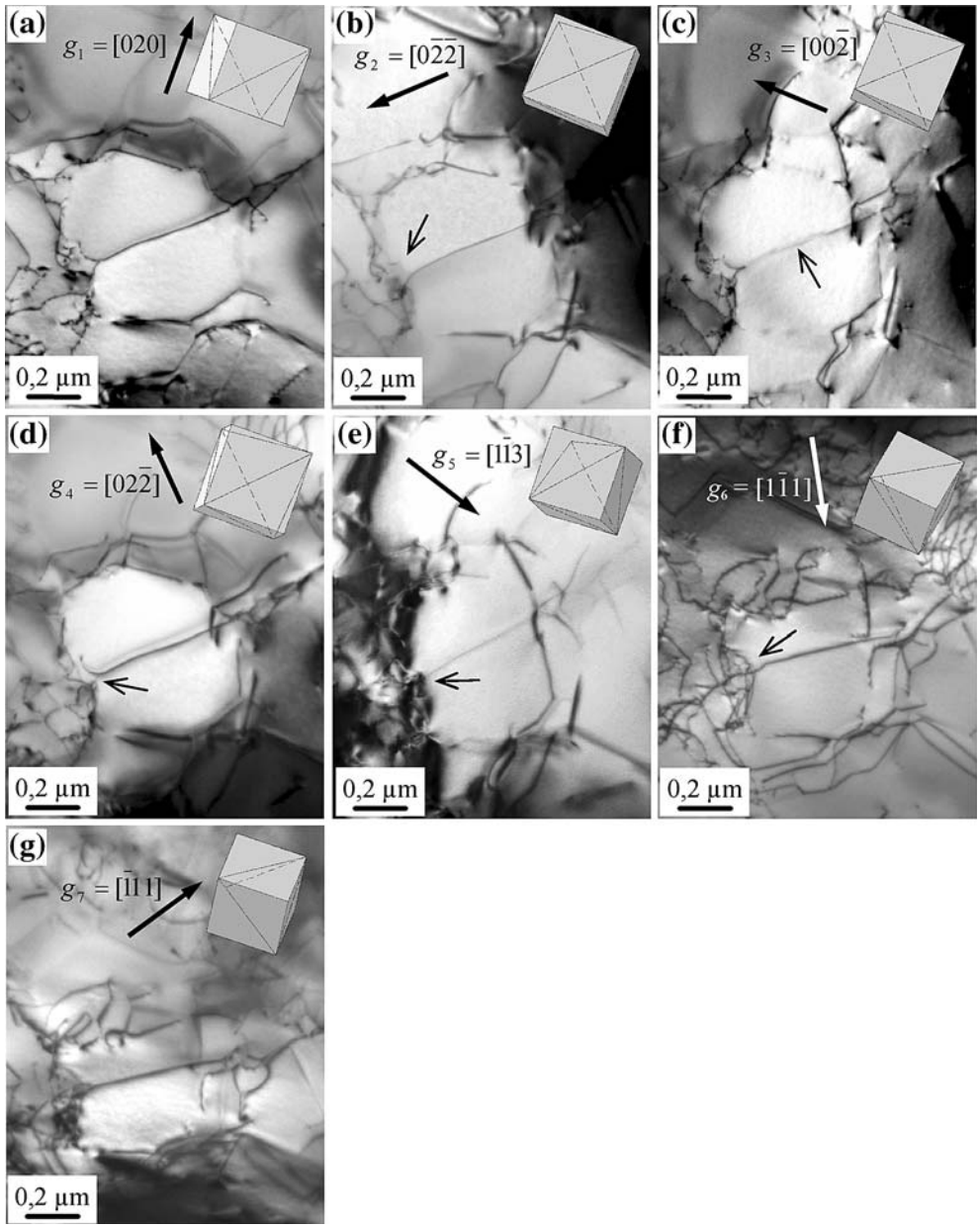

Fig. 5 TEM micrographs showing the cutting of a γ'-particle after ⟨100⟩ tensile creep at 980 °C and 240 MPa. All dislocation segments are referred to as outlined in Fig. 3. (**a**) $g_1 = [020]$: all dislocation segments are visible; (**b**) $g_2 = [0\bar{2}\bar{2}]$: dislocation segment $d_{\gamma 1}$ (arrow) is invisible; (**c**) $g_3 = [00\bar{2}]$: superdislocation segment $d_{\gamma'}$ (arrow) exhibits weak residual contrast; (**d**) $g_4 = [00\bar{2}]$: dislocation segment $d_{\gamma 2}$ (arrow) is invisible; (**e**) $g_5 = [1\bar{1}3]$: dislocation segment $d_{\gamma 2}$ is invisible; (**f**) $g_6 = [1\bar{1}\bar{1}]$: dislocation segment $d_{\gamma 1}$ (arrow) is invisible; (**g**) $g_7 = [\bar{1}11]$: all dislocation segments are visible

Table 2 Burgers vectors and line directions for the superdislocation segments marked in Fig. 3

Dislocation segment	Burgers vector **b**	Dislocation line direction **u**
$d_{\gamma'}$	$\pm a[010]$	$1/\sqrt{2}[010]$
$d_{\gamma 1}$	$\pm a/2[21\bar{1}]$	$1/\sqrt{101}[6\bar{1}8]$
$d_{\gamma 2}$	$\pm a/2[\bar{2}11]$	$1/\sqrt{41}[1\bar{6}\bar{2}]$

each of the γ-channel dislocations $d_{\gamma 1}$ and $d_{\gamma 2}$ which show that they have Burgers vectors $\mathbf{b}_{d\gamma 1} = \pm a/2[21\bar{1}]$ and $\mathbf{b}_{d\gamma 2} = \pm a/2[\bar{2}11]$. The superdislocation line segment is never effectively invisible. For one contrast condition, it shows residual contrast. However, since the two channel dislocations $d_{\gamma 1}$ and $d_{\gamma 2}$ combine to form the superdislocation $d_{\gamma'}$ we can obtain its Burgers vector from a reaction

$$\pm a/2([21\bar{1}] + [\bar{2}11]) = \pm a[010].$$

This suggests that the resulting superdislocation has a Burgers vector of type $\pm a[010]$. This result needs to be discussed in view of the residual contrast which we obtain for a **g** of $[00\bar{2}]$ in Fig. 5c. Both **b** and $\mathbf{b} \times \mathbf{u}$ of the superdislocation are perpendicular to this reflection vector **g** and therefore one may expect effective invisibility. The residual contrast in Fig. 5c may be

Table 3 Visibility and invisibility of all analysed dislocations and determined Burgers vectors; res.: residual contrast

Dislocation	**g**1 [020]	**g**2 $[0\bar{2}\bar{2}]$	**g**3 $[00\bar{2}]$	**g**4 $[02\bar{2}]$	**g**5 $[1\bar{1}3]$	**g**6 $[1\bar{1}1]$	**g**7 $[\bar{1}11]$	Burgers vector **b**
$d_{\gamma'}$	+	+	res.	+	+	+	+	$\pm a[010]$
$d_{\gamma 1}$	+	–	+	+	+	–	+	$\pm a/2[21\bar{1}]$
$d_{\gamma 2}$	+	+	+	–	–	+	+	$\pm a/2[\bar{2}11]$

associated with a split superdislocation core where two superpartials with a disordered region in between jointly shear the γ'-particle. It may moreover be related to an elastic anisotropy of the $L1_2$-phase. Even in case of a compact dislocation core an anisotropic displacement field can give rise to a weak residual contrast. Further work is required to clarify this point. It is important for the present work to highlight that the residual contrast in Fig. 5c does not exclude the possibility that the superdislocation $d_{\gamma'}$ has a Burgers vector of type $\pm a[010]$. The results presented so far support our previous findings in [12, 14] and the recent results by Zhang et al. [17]. They clearly show that two γ-channel dislocations with different Burgers vectors can join to form a superdislocation which shears the γ'-particle. In the case of the present study, this linear defect is a 45° superdislocation with a Burgers vector of a [010]. It is a new observation that the two γ-channel dislocations have Burgers vectors of type $\langle 211 \rangle$.

Figure 6a and b show TEM-micrographs taken for **g**s of $[00\bar{2}]$ and $[02\bar{2}]$ at a higher magnification in the region where the γ-channel dislocations cut into the γ'-particle. Both micrographs clearly show that dislocation $d_{\gamma 2}$ results in fact from a reaction between two other γ-channel dislocations. This situation could not be observed under a sufficient number of diffraction conditions to directly identify the Burgers vectors of these two channel dislocations. But it seems reasonable to assume that these two dislocations are of type $\langle 110 \rangle$ and form the dislocation $d_{\gamma 2}$ according to a reaction of type

$$a/2[\bar{1}10] + a/2[\bar{1}01] = a/2[\bar{2}11].$$

In the case of γ-channel dislocation $d_{\gamma 1}$, it seems reasonable to assume that this dislocation segment forms according to a reaction

$$a/2[110] + a/2[10\bar{1}] = a/2[21\bar{1}].$$

The results presented in Figs. 5 and 6 prove that high temperature γ'-cutting by γ-channel dislocations with different Burgers vectors can also be observed in the single crystal superalloy LEK94. Since this type of cutting process has now been observed in CMSX-6 [12, 13], CMSX-4 [14], TMS-138 [17] and LEK94 (present study) it seems reasonable to assume that it represents a generic dislocation processes which governs high temperature plasticity under conditions of high temperature and low stress creep in γ/γ'-microstructures of Ni-base single crystal superalloys. It has been shown that these superdislocations have split cores and can only move by a combined process of glide and climb [12, 14]. As a new result it was observed that the two channel dislocations $d_{\gamma 1}$ and $d_{\gamma 2}$ can also form in reactions between γ-channel $\langle 110 \rangle$-dislocations. Figure 7 provides a 3D illustration which rationalizes the dislocation processes that were observed in the present work. It shows that the $\pm a[010]$ superdislocation can result from the combination of two $\langle 211 \rangle$-type dislocations which in turn form by reactions between $\langle 110 \rangle$-dislocations. In this sense dislocation reactions can be even more complex than was previously observed [12, 14].

Alloy chemistry certainly is important and governs key microstructural parameters like lattice misfit, anti phase boundary energy in the γ'-phase and others. But the fact that high temperature cutting of the γ'-phase by two γ-channel $\langle 110 \rangle$-dislocations with different Burgers vectors has now been documented for four single crystal super alloys with different alloy chemistry (CMSX-6, CMSX-4, TMS-138 and LEK94) suggests that alloy chemistry is less important with respect to the operation of this type of cutting process.

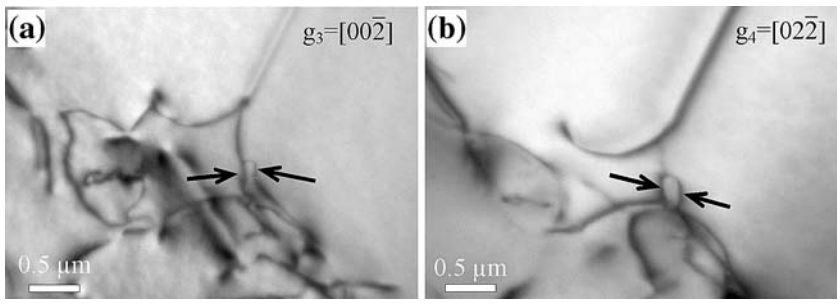

Fig. 6 The γ/γ' interface region observed in high magnification at two different tilt positions. Reactions of previously analysed dislocation $d_{\gamma 2}$ with other γ-channel dislocation segments are marked by arrows

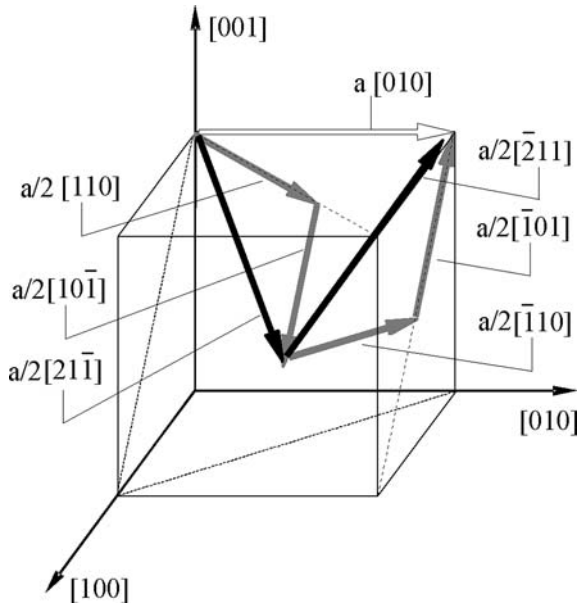

Fig. 7 Schematic diagram illustrating the dislocation processes that were observed in the present work. An a [010] superdislocation can result from the combination of two ⟨211⟩-type dislocations which form by reactions between ⟨110⟩-dislocations

Summary and conclusions

In the present work, we study the cutting of a γ'-particle in the Ni-base single crystal superalloy LEK94 under conditions of high temperature and low stress creep. From the results obtained the following conclusions can be drawn:

(1) Two γ-channel dislocations with different Burgers vectors combine: ($\pm a/2([21\bar{1}] + [\bar{2}11]) = \pm a[010]$) to form a superdislocation which shears the γ'-particle. This type of cutting process has been recently observed in two other Ni-base single crystal superalloys. It therefore is concluded that it represents a generic feature of high temperature and low stress creep in this class of materials.

(2) The Burgers vectors of the two γ-channel dislocations were identified as $\mathbf{b}_{d\gamma 1} = \pm a/2[21\bar{1}]$ and $\mathbf{b}_{d\gamma 2} = \pm a/2[\bar{2}11]$. It was observed that they can represent reaction products resulting from dislocation reactions of type

$$a/2[\bar{1}10] + a/2[\bar{1}01] = a/2[\bar{2}11]$$
$$\text{and } a/2[110] + a/2[10\bar{1}] = a/2[21\bar{1}]$$

This represents a new observation and suggests that under conditions of high temperature and low stress creep more complex dislocation reactions in the γ-channels may precede the formation of a $\pm a[010]$ superdislocation in the γ'-particle.

(3) With the results obtained in the present work, dislocation processes where two γ-channel dislocations with different Burgers vectors jointly shear the γ'-phase have now been observed for four single crystal Ni-based super alloys with varying alloy composition, including CMSX-4, CMSX-6 TMS-138 and LEK94 (present work). This suggests that this type of γ'-cutting is a generic high temperature dislocation process which may well govern the creep rate of the whole family of Ni-base single crystal super alloys and which is not strongly dependent on variations in alloy chemistry.

Acknowledgements The authors acknowledge funding by the Deutsche Forschungsgemeinschaft (DFG) under contract EG 101/9.

References

1. Meetham GW (1981) The development of gas turbine materials. Applied Science Publishers, London, p 1
2. McLean M (1983) Directionally solidified materials for high temperature service. The Metals Society, London
3. Leopold J (1984) Gasturbinen. In: Allianz-Handbuch der Schadensverhütung. VDI-Verlag, Berlin, p 349
4. Pollock TM, Argon AS (1992) Acta Metall Mater 40:1
5. Mayr C, Eggeler G, Dlouhy A (1996) Mater Sci Eng A207:51
6. Gleiter H, Hornbogen E (1965) Acta Metall 13:576
7. Gleiter H, Hornbogen E (1965) Phys Status Solidi 12:251
8. Gleiter H, Hornbogen E (1967) Z Metallkd 58:157
9. Nabarro FRN, de Villiers HL (1995) The physics of creep. Taylor & Francis, London, p 103
10. Louchet F, Ignat M. (1986) Acta Metall 34:1681
11. Bonnet R, Ati A (1989) Acta Metall 37:2153
12. Eggeler G, Dlouhy A (1997) Acta Mater 45:4251
13. Dlouhy A, Schäublin R, Eggeler G (1998) Scripta Mater 39:1325
14. Srinivasan R, Eggeler G, Mills MJ (2000) Acta Mater 48:4871
15. Epishin A, Link T (2004) Phil Magn 84:1979
16. Zhang JX, Wang JC, Harada H, Koizumi Y (2005) Acta Mater 53:4623
17. Zhang JX, Harada H, Koizumi Y (2006) J Mat Res 21:647
18. Kamaraj M (2003) Sadhana-academy proceedings in engineering sciences vol 28, p 115
19. Murken J, Serin K, Eggeler G (2001) Proceedings of Baltica V. In: Hietanen S, Auerkari P (eds) International conference on condition and life management for power plants, Porvo, Finland, June 2001. VTT Technical Research Centre of Finland, Espoo, p 583
20. Skrotzki B, Neuking K, Mayr Ch, Eggeler G (1998) Mat-wiss u Werkstofftech 28:137
21. Hirsch PB, Howie A et al (1965) Electron microscopy of thin crystals. Butterworths, London, p 121
22. Edington JW (1976) Practical electron microscopy in materials science. Van Nostrand Reinhold, Eindhoven, p 118
23. Dlouhy A, Eggeler G (1996) Prakt Metall 33:629